Rapidly solidified structure of alloys with up to eight equal-molar elements—a simulation by molecular dynamics

2008 J. Phys.: Condens. Matter 20 145214

(http://iopscience.iop.org/0953-8984/20/14/145214)

J. Phys.: Condens. Matter **20** (2008) 145214 (7pp) doi:10.1088/0953-8984/20/14/145214

Rapidly solidified structure of alloys with up to eight equal-molar elements—a simulation by molecular dynamics

Su-Wen Kao[1], **Jien-Wei Yeh**[1] **and Tsung-Shune Chin**[1,2,3]

[1] Department of Materials Science and Engineering, National Tsing Hua University, 101, Section 2, Kuang-Fu Road, Hsinchu 30013, Taiwan, Republic of China
[2] Department of Materials Science and Engineering, Feng Chia University, 100, Wenhwa Road, Seatwen District, Taichung 40724, Taiwan, Republic of China

E-mail: d907523@oz.nthu.edu.tw, jwyeh@mx.nthu.edu.tw and tschin@fcu.edu.tw

Received 30 August 2007, in final form 3 February 2008
Published 19 March 2008
Online at stacks.iop.org/JPhysCM/20/145214

Abstract

Alloys with equal-molar elements (so-called high-entropy alloys) designed since 1995 are unique in many aspects and possess extraordinary structural and functional properties. In this study, structure evolutions were simulated for alloys with two to eight equal-molar elements Ni, Al, Cu, Co, Ti, V, Zn, Zr (in sequence) as being molten, rapidly solidified (at 2×10^{13} K s^{-1}), and annealed at 900 K, respectively. The simulation was done using molecular dynamics with tight-binding potential energy and the Verlet algorithm, taking into consideration the difference in crystal structure and atomic size of the constituent elements. The obtained radial distribution function (RDF) was quantitatively analyzed. Three factors obviously dominating are the number of elements (n), the size of constituent elements, and temperature. For n less than four the melt-quenched alloys tend to form amorphous structure; however, when n is five and more, the alloys show a liquid-like solidified structure. The annealing at 900 K results in a higher degree of order for amorphous structure in alloys with $n \leqslant 6$, while it makes alloys with $n \geqslant 7$ more random than those of their original quenched state. The hard ball model is proposed to explain the evolution of amorphous and liquid-like structures. The mechanism of the annealing effect is elucidated by the competition between the dense packing (for lowering enthalpy energy) and the randomness of atoms (for increasing $T\Delta S$) driven by thermal energy.

1. Introduction

In 1995, one of the co-authors, Yeh, proposed for the first time an approach of alloy design [1], in which alloys are attained without any dominant element. This is completely different from conventional alloys used since human civilization based on a specific principal element such as Cu in Cu alloys and Fe in steels, etc. In this approach, a number of constituent elements, n, satisfying $5 \leqslant n \leqslant 13$ are recommended and the atomic concentrations of the jth element, c_j, are in equal-mole basis. Moreover, they can be further extended to satisfy a wider range: 5 at.% $\leqslant c_j \leqslant$ 35 at.% for the optimization of properties. Such alloys were named 'high-entropy alloys' (HEAs) due to their inherently higher configurational entropies. According to this definition of HEAs, counting 80 available metallic elements, there will be a total of 7099 HEA systems [2–4], a number too huge to work out through iterating experiments. A simulation technique, such as molecular dynamics [5], is a way to screen suitable HEA systems worthy of experimental trials. This study exemplifies such a trial.

Several HEA alloys have been worked out with excellent performances. Yeh *et al* disclosed distinguished structural and mechanical properties of alloys based on the Cu–Co–Ni–Cr–Al–Fe–Ti–V system [6]. Thin films of Fe–Co–Ni–Cr–Cu–Al–Mn and Fe–Co–Ni–Cr–Cu–$Al_{0.5}$ were sputter-deposited on a silicon substrate under nitrogen containing atmosphere to form nitride films with much improved hardness and thermal stability [7]. Lots of other HEAs with performances much better than those of conventional alloys have been

[3] Author to whom any correspondence should be addressed.

evidenced [8–17]. In general, an experienced metallurgist will predict, instinctively, that many intermetallic phases will form when a lot of metallic elements are melted together. Yet this is not the true case. HEAs are solid-solution phases possessing simple crystal structures (fcc, bcc) and/or amorphous phases, despite the fact that a large number of elements are involved. They usually have much better high temperature performances, such as the resistance to temper-softening and extraordinarily high hardness at temperatures higher than 800 °C, to name just a few. This is mainly contributed from the much larger $T\Delta S$ value in Gibbs free energy ($\Delta G = \Delta H - T\Delta S$) at high temperatures.

The molecular dynamics simulation method is a powerful tool in materials research, and has been widely used to provide an atomic description of the crystallization and glass forming processes during rapid solidification of alloys. The quantum mechanics based many-body tight-binding potential model is utilized to represent the inter-atomic forces existing among atoms in MD simulation.

Tomanek [18] published the second moment approximation of tight-binding molecular dynamics from the tight-binding scheme, which is based on a small set of adjustable parameters, and, at least in principle, is suitable for extension to high moments of the electronic density of states. The tight-binding model commences by summing the band energy, which is characterized by the second moment of the d-band density of states, and a pair-wise potential energy of the Born–Mayer type. Even though it seems similar to the EAM (embedded atom method) potential, the tight-binding potential yields more accurate predictions of some characteristics of certain transition metals than that of the EAM. 'Tight-binding MD' well describes behaviors of metals specifically for transition metals. Among many scientists who contributed to the calculation method, Cleri and Rosato summarized the tight-binding parameters and some calculation results in 1993 [19]. Several tight-binding MD simulations have been published to demonstrate structural and thermodynamic behaviors of alloys, to name just a few, by Duan *et al*, on $Cu_{46}Zr_{54}$ alloy [20]; by Ferrando *et al*, who explored the diffusion of Au on Ag(111) [21]; and by Guerdane *et al*, who studied ternary $Ni_{25}Zr_{60}Al_{15}$ alloy [22]. This was the reason why we used the tight-binding model and Verlet algorithm to explore behaviors of alloys with multiple transition metals.

2. Simulation method

Based on the tight-binding model [19], the energy of a single atom can be divided into two parts, being its attractive and repulsive components. The attractive potential (E_B^i) is given by

$$E_B^i = -\left\{\sum_j \xi_{\alpha\beta}^2 \exp\left[-2q_{\alpha\beta}\left(\frac{r_{ij}}{r_0^{\alpha\beta}} - 1\right)\right]\right\}^{1/2} \quad (1)$$

where r_{ij} represents the distance between atoms i and j, r_0 is the first-neighbor distance, ξ is an effective hopping integral and q describes its dependence on the relative inter-atomic distance, α and β are the different lattices of unlike neighboring atoms, and both $q_{\alpha\beta}$ and $\xi_{\alpha\beta}$ are the geometrical average of these atoms in α and β lattices, respectively.

Table 1. Relative information on tight-binding parameters [19].

	Structure	r_0 (Å)[a]	Atomic mass	A (eV)	ξ (eV)	p	q
Ni	fcc	2.50	58.6934	0.0376	1.07	16.999	1.189
Al	fcc	2.86	26.9815	0.1221	0.1221	8.612	2.516
Cu	fcc	2.56	63.546	0.0855	1.224	10.96	2.278
Co	hcp	2.50	58.9332	0.098	1.488	11.608	2.286
Ti	hcp	2.92	47.867	0.1519	1.8112	8.62	2.39
V	bcc	2.70	50.9415	0.6124	2.441	5.206	1.22
Zn	hcp	2.78	65.39	0.1477	0.89	9.689	4.602
Zr	hcp	3.20	91.224	0.1934	2.2792	8.25	2.249

[a] r_0 indicates the atomic diameter of each element.

The repulsive interaction term is normally assumed to be pair-wise, and described by a sum of Born–Mayer ion–ion repulsions:

$$E_R^i = \sum_j A_{\alpha\beta} \exp\left[-p_{\alpha\beta}\left(\frac{r_{ij}}{r_0^{\alpha\beta}} - 1\right)\right]. \quad (2)$$

The parameter, p, is related to the compressibility of the bulk metal. A is dependent on the experimental values of the lattice parameter. In brief, the four parameters (ξ, A, p and q) are fitted to known bulk properties of the crystals, that are the experimental values of cohesive energy, lattice parameter, bulk modulus and elastic constants.

The parameters of elements studied are shown in table 1. According to these parameters, all possible combinations that the elements of the system can have are considered, and then the geometric mean is applied for $q_{\alpha\beta}$, $\xi_{\alpha\beta}$, $A_{\alpha\beta}$ and $p_{\alpha\beta}$, whereas the arithmetic mean is applied for $r_0^{\alpha\beta}$.

The total cohesive energy of the system is then, with the band quantum mechanics in origin, incorporating a many-body summation,

$$E_C = \sum_i (E_R^i + E_B^i). \quad (3)$$

The MD simulations for the present HEA systems were carried out in a cubic super-cell containing 4000 atoms, under a constant pressure condition (zero applied pressure) and under periodic boundary conditions. Each time step used was 1×10^{-15} s during the simulation process.

In the present study, binary to eight-element alloys, with the elements in equimolar proportion and in the sequence of Ni, Al, Cu, Co, Ti, V, Zn, and Zr, i.e. Ni–Al binary alloy, Ni–Al–Cu ternary alloy, Ni–Al–Cu–Co quaternary alloy etc, were examined using MD simulation. In addition, single elements, V, Co and Ni, were simulated likewise for further comparison.

Thermal history in the present MD simulation is shown in figure 1. First, the mixture of 4000 atoms from the elements under consideration was put in a cubic cell and run with 15 000 steps (1×10^{-15} s/step, so a total of 15 ps) at 300 K. After heating up to 2200 K at the rate of 2×10^{13} K s^{-1} and holding for 15 ps, the system was quenched at a rate of 2×10^{13} K s^{-1} to 300 K from the molten state. All mixtures were initially set to have the same cubic cell size at 300 K. After quenching, post-annealing was performed at 900 K on the melt-quenched

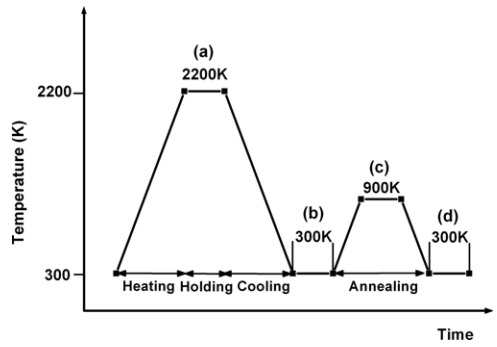

Figure 1. Thermal history of studied alloys.

alloys. The quenching rate of 2×10^{13} K s^{-1} was also used for cooling from the annealing temperature to 300 K. The stages shown in figure 1 thus include (a) the molten state, (b) the melt-quenched state (quenching from the melt to 300 K), (c) the annealing state at 900 K and (d) the annealed state quenching from 900 to 300 K. The alloys were held for 15 ps at each stage for better homogeneity and stability.

3. Results

Figures 2 and 3 show the calculated radial distribution function (RDF) of alloys, and single elements V, Co, Ni, respectively, at the various stages presented in figure 1. Here, RDF represents the real-space distribution function in which density function $\rho(r)$ is divided by the average atomic density ρ_0. All the liquid phase has broad and well defined first and second peaks in the RDF pattern, shown in figures 2(A) and 3(A). The higher-order peaks, however, fade away quickly. This is representative of the disorder expected in liquid metals, and shall be taken as the reference for other states. Both single elements with different crystal structures and the multi-element alloys show similar behavior at the molten stage.

Figure 2(B) shows RDFs of multi-element alloys in the melt-quenched state. The second RDF peak of alloys with n (the number of elements) four and less is split, which is indicative of amorphous structure [23]. However, the melt-quenched structure obtained for alloys with $n = 5$ (Ni–Al–Cu–Co–Ti) to $n = 8$ (Ni–Al–Cu–Co–Ti–V–Zn–Zr) is liquid-like, similar to those of molten alloys, since their second peaks in RDFs are not split. This demonstrates that the alloys containing five and more equimolar elements have a strong tendency to possess a liquid-like structure after quenching, as compared to the amorphous structure obtained by alloys with a smaller number of elements. This phenomenon matches surprisingly well with Yeh's definition of HEAs.

From a comparison among RDF patterns in figure 2(B) versus (C), it is seen that, as a result of thermal annealing, the melt-quenched RDF patterns change very little for alloys containing two to four elements but significantly for alloys of higher n. For the five- and six-element alloys the first peak becomes narrower and the second peak becomes split, whereas for seven- and eight-element alloys the first and the second peaks become more diffuse. This implies that the thermal energy gained during annealing at 900 K is not enough to vary much the amorphous structure toward crystalline structure

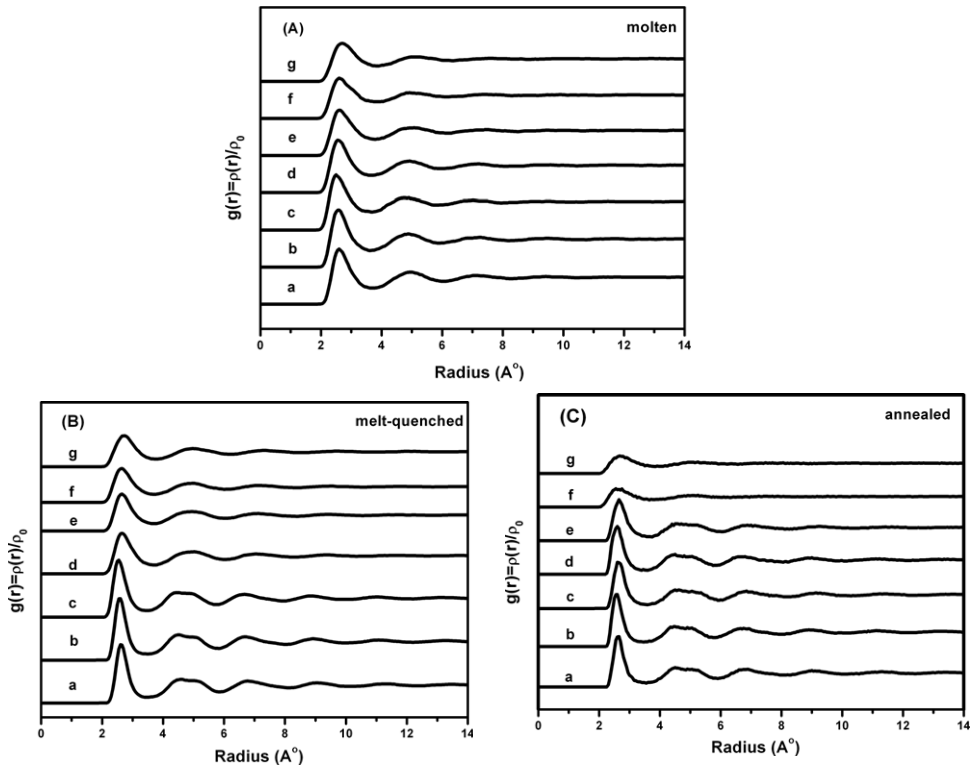

Figure 2. Calculated RDF patterns of the alloys: (A) in the molten state; (B) in the melt-quenched state; (C) in the annealed state. a, Ni–Al; b, Ni–Al–Cu; c, Ni–Al–Cu–Co; d, Ni–Al–Cu–Co–Ti; e, Ni–Al–Cu–Co–Ti–V; f, Ni–Al–Cu–Co–Ti–V–Zn; g, Ni–Al–Cu–Co–Ti–V–Zn–Zr.

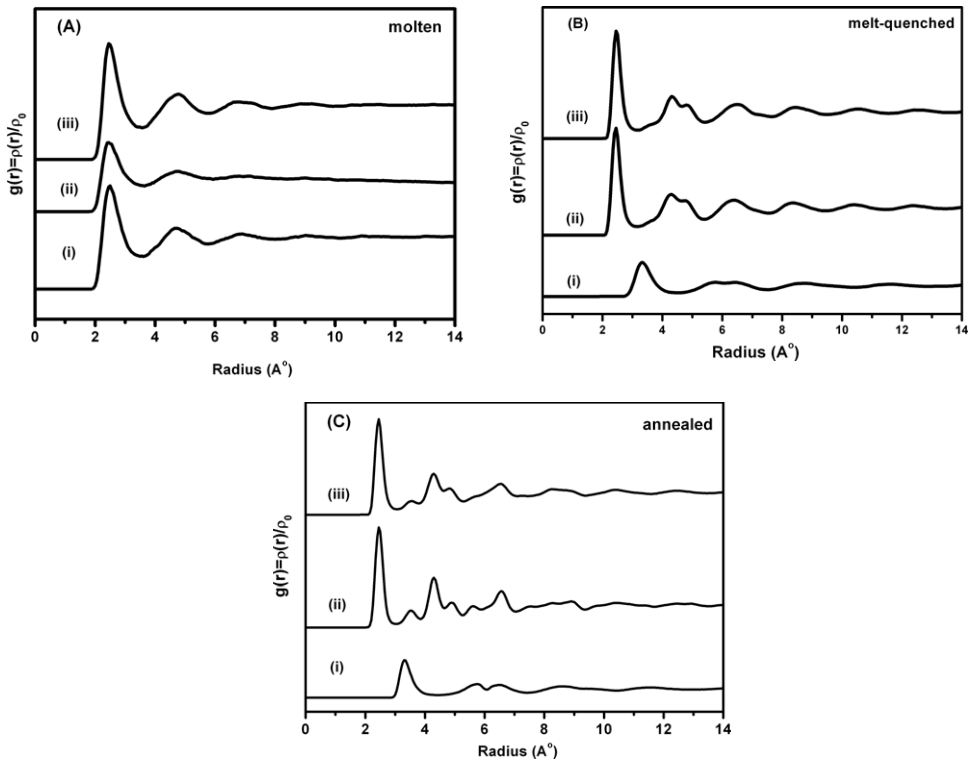

Figure 3. Calculated RDF patterns of single elements: (A) in the molten state; (B) in the melt-quenched state; (C) in the annealed state. i, V; ii, Co; iii, Ni.

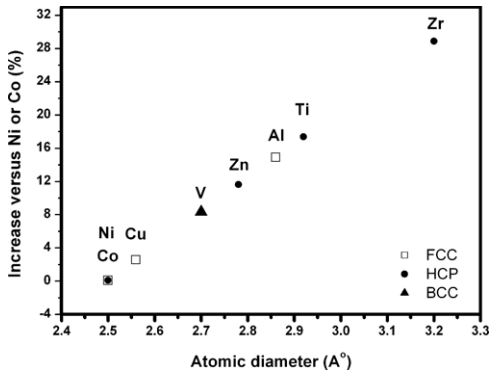

Figure 4. Distribution of atomic radius and structure for the eight experimental elements.

for two- to four-element alloys but enough for five- and six-element alloys to change from liquid-like to amorphous structure. In contrast, the thermal energy at 900 K is not able to change the liquid-like structure into an amorphous one on seven- and eight-element alloys, but on the contrary results in a liquid-like structure with a higher degree of disorder.

Further supports for the above trend are seen from RDF patterns of single elements V, Co and Ni with different crystal structures. In the molten state shown in figure 3(A), all the RDF curves show the typical pattern of a liquid structure similar to those alloys noted above. Although it is extremely difficult to obtain amorphous state for single metallic elements through the existing rapid melt-quenching method in a practical range of cooling rate 10^3–10^9 K s^{-1}, it has been reported that certain metallic elements such as Ni, Co, Mn, Cr and Fe are amorphous by thermal evaporation on substrates held at very low temperatures such as 4 K (the quench rate is equivalent to the order of 10^{12-13} K s^{-1}) [24, 25]. In the melt-quenched state shown in figure 3(B), the first peak becomes narrower and the second peak does split, indicating an amorphous structure. In the annealed state shown in figure 3(C), V, Co and Ni become crystalline. The annealing effect is obviously more pronounced than that observed in two- to four-element alloys. All these structures are fitted with the trends influenced by the number of elements observed in figure 2.

4. Discussion

4.1. HEA design

By increasing the degree of disorder of the HEA system, the Ni–Al–Cu–Co–Ti–V–Zn–Zr system is selected purposely based on fcc (Ni, Al and Cu) structure, with hcp-structured elements added (Co and Ti), then the bcc-structured element (V) and finally hcp-structured Zn and Zr [26]. This was designed to explore the effect of the variation in atomic structure and size on the rapid-quenched HEA alloys. To be more specific, figure 4 shows the atomic size and structure distribution. The ordinate is the increase in atomic size based on the diameter of Ni or Co (same size). The square symbol represents fcc, circle hcp and triangle stands for bcc structure. One example is given here, for instance, $(R_V - R_{Co})/R_{Co} = (2.7 - 2.5)/2.5 = 8\%$. From the atomic size difference as

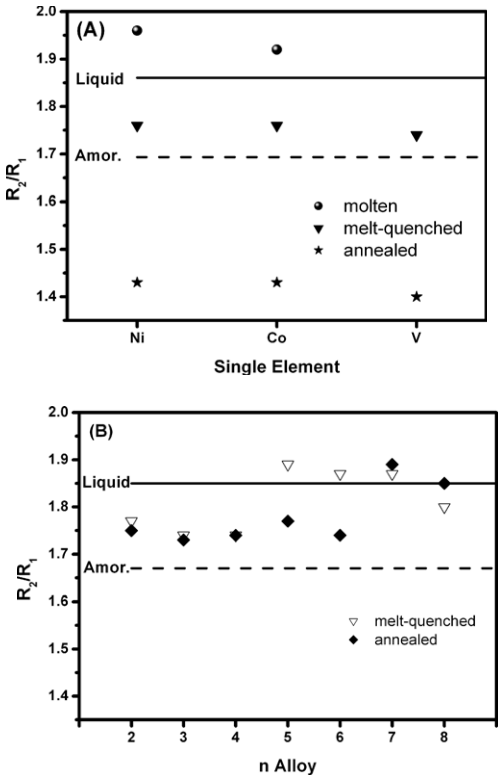

Figure 5. Calculated R_2/R_1 values for (A) single elements and (B) equimolar alloys.

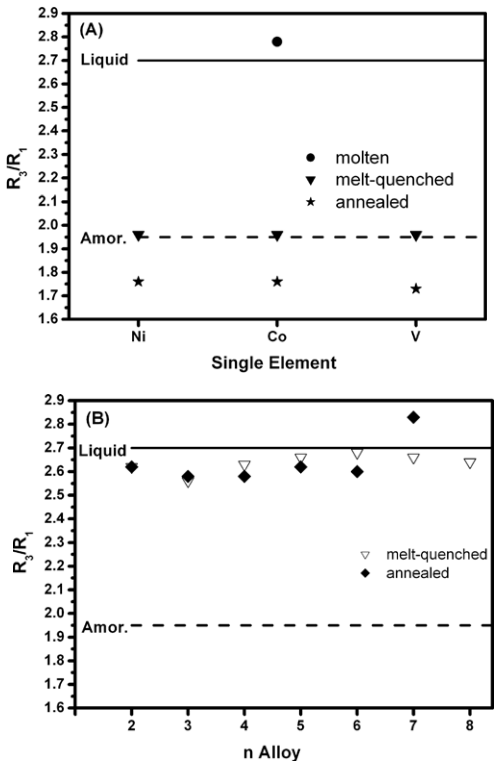

Figure 6. Calculated R_3/R_1 values for (A) single elements and (B) equimolar alloys.

shown in the figure, the largest size variation of this HEA alloy is 32%. It was expected that randomness and free volume can be introduced through this variety of elements chosen.

4.2. Peak-broadening and peak-position ratio

The peak-broadening and peak-position ratio deserve quantitative analyses. In the molten state shown in figures 2(A) and 3(A), it can be seen that the first peak becomes broader with increasing number of elements. In the melt-quenched and annealed state, a similar trend is observed except for the significant narrow-down of the first peak due to the large reduction of free volume and thermal energy as compared with that at the molten state. This reflects the variation in atomic size with structure for multicomponent alloys and will be further discussed in the next section.

In accordance with the definition used by Waseda [23], the position of the first peak is defined as R_1, that of the unsplit second peak as R_2, that of the third peak as R_3 and so on. However, in the case of a split second peak, the distance of the front small peak is defined as R_2, that of the rear small peak as R_3 and so on. The ratios of R_2/R_1 and R_3/R_1 have principal structural significance. As deduced in the reference by Waseda [23], the R_2/R_1 and R_3/R_1 values are 1.67 and 1.95 for an amorphous solid, and 1.85 and 2.70 for a liquid, respectively [23]. The variations in R_2/R_1 and R_3/R_1 are plotted in figures 5 and 6. Let us start from the single elements in the molten and melt-quenched states. Figure 5(A) shows that the R_2/R_1 values of the three single elements, Ni, Co and V, in the melt-quenched state are close to each other and a little higher than the 1.67 (amorphous structure) predicted by Waseda [23]. In the annealed state, their R_2/R_1 values fall to that for crystalline structure. Figure 5(B) shows the variation in R_2/R_1 value with n of HEA. As $n \leqslant 4$, the degree of disorder in the melt-quenched state is almost the same as those of single elements and close to the line denoting the amorphous state, whereas the degree of disorder in the annealed state is unlike those of single elements and almost remains at a similar level. As $n = 5$ and 6, the melt-quenched R_2/R_1 values are higher than the line denoting liquid, while after the 900 K annealing, R_2/R_1 values resume those of the amorphous state. This means that 900 K annealing does eliminate some of the quenched randomness of the liquid-like structure for the alloys with $n = 5$ and 6. It is overwhelming that for alloys with $n = 7$ and 8 the R_2/R_1 values are not lowered by the 900 K annealing. To our great surprise, on the contrary, the R_2/R_1 value is increased a little more than that of their original liquid structure due to the 900 K annealing. That is to say, the 900 K annealing bestows even more randomness than that of the melt-quenched state. These variations can only be explained by the much enhanced configurational entropy effect for the alloys with $n = 7, 8$ versus those with $n \leqslant 6$, which will be further discussed in the next section.

Then let us take a look at the variation in the value of R_3/R_1. Figure 6(A) shows the variation of the values for the single elements, Ni, Co, and V. In the melt-quenched state, their R_3/R_1 values are equal exactly to the definition line of amorphous structure, being consistent with that shown in figure 5(A). In the annealed state, crystallization is also observed as expected. Figure 6(B) shows the variation in

R_3/R_1 value with n of HEAs. In the melt-quenched state, the R_3/R_1 values of all the alloys are found to be close to the definition of liquid-like structure. In comparison with that found from figure 5(B) in which only alloys with $n \geqslant 5$ fulfill the condition of liquid-like structure, this implies that alloys with $n = 2$–4 in the melt-quenched state have an amorphous structure with a higher degree of disorder than the standard amorphous structure. In the annealed state, alloys with $n = 2$–6 have their R_3/R_1 values similar to that of their original structure, but for the alloy with $n = 7$ the third RDF peak flattens to be hardly identifiable and for $n = 8$ it is not identifiable. This is consistent with that observed in figure 5(B). The 900 K annealing bestows even more randomness than that of the melt-quenched state.

4.3. Hard ball model explaining the effects of the number of elements, atomic size difference and annealing on amorphization

From the simulation results, it has been revealed that the number of elements, atomic size difference and annealing have their significant effects on the atomic configuration. In the molten state shown in figures 2(A) and 3(A), it has already been seen that the first peak becomes broader with increasing number of elements. In the melt-quenched and annealed states, a similar trend is observed. Based on the hard ball model this indicates that a larger variety of atomic size (resulting from a larger number of different elements) causes more diffuse or distorted (due to atomic size difference) first shell, second shell and so on. Moreover, since the second and third shells, and also the fourth and fifth shells, are quite close in space, it is expected that a certain degree of shell diffusion renders them indistinguishable from each other. Then, this will result in a liquid-like structure or amorphous structure depending on whether the second and third shells are distinguishable or not. In contrast to a crystal structure which has many sharp RDF peaks corresponding to the first, second, third, fourth, fifth shells and so on, a liquid-like structure has broad and attenuated peaks in which the broad second peak is due to the merging of the second and third shells, and the third broad peak is due to that of the third and fourth shells. On the other hand, an amorphous structure has a split second peak reflecting the partial merging of the second and third shells, and the third broad peak reflecting the merging of the third and fourth shells. Figure 7 depicts a hard ball close packing model of a liquid-like atomic packing structure using multiple elements of different sizes. The circles represent the first, second, third, fourth and fifth shells, respectively, but the second and third shells are indistinguishable due to the large atomic size difference and thus the large fluctuation in occupation of different atoms. The fourth and fifth shells are also indistinguishable. The phenomena that increased number of elements has a stronger tendency to give a topological-disorder-like amorphous structure and even a liquid-like one as revealed by the simulation results could thus be explained by this hard ball model. This also provides a way to verify the confusion principle proposed by Turnbull [27, 28] and Greer [29]. The principle means that more components to constitute an alloy will have a lower chance to select viable crystal structures and thus have greater glass formability.

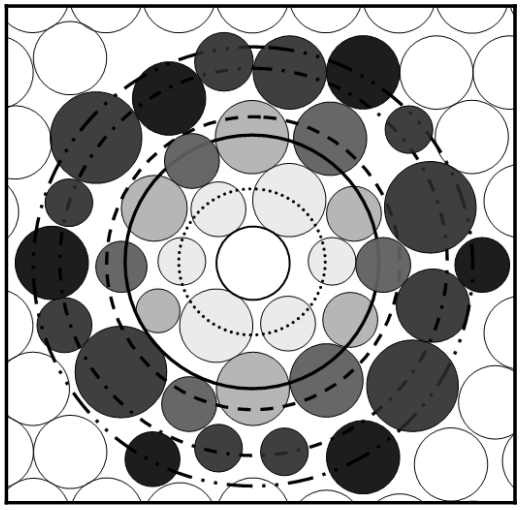

Figure 7. A hard ball model of a liquid-like atomic packing structure using multiple elements of different sizes. The circles represent the first, second, third, fourth and fifth shells, respectively, but the second and third shells are indistinguishable due to the large atomic size difference and thus the large fluctuation in occupation of different atoms. The fourth and fifth shells are also indistinguishable.

However, the hard ball model is especially suitable for the topological instability of crystal structure under the conditions without chemical short-range order. It is enough for the present simulation since the geometric mean was applied for $q_{\alpha\beta}$, $\xi_{\alpha\beta}$, $A_{\alpha\beta}$, and $p_{\alpha\beta}$, whereas the arithmetic mean for $r_0^{\alpha\beta}$ in the potential equations (1) and (2), implying that the bonding energy of all unlike atomic pairs is zero like those in an ideal solution. The present simulation thus provides an advantage to isolate and clarify the effects of the number of elements, atomic size, and thermal treatment without the interference of the effect due to the excess bonding energies between unlike atoms. Obviously, the actual liquid-like or amorphous structure might be influenced by chemical short-range order. For such structures, Bernal's dense random packing of hard spheres could be satisfactorily used for alloys with constituent atoms having comparable atomic sizes and insignificant chemical short-range order [30, 31]. For larger difference in atomic sizes and/or chemical short-range order such as metal–metalloid systems and bulk metallic glasses, a canonical collection of efficiently packed hard ball sphere clusters including solute-centered and solvent-centered atomic clusters proposed by Miracle *et al* is a good description [32, 33]. Besides, short-range order of different types of solute-centered clusters or coordination polyhedra, and medium-range order of the packing of polyhedra obtained with *ab initio* molecular dynamics simulation by Ma *et al*, provides a good model to elucidate the effects of different chemistry and atomic size ratios of constituent atoms [31].

As for the annealing effect, it has been concluded from the comparison of RDF patterns that the structure of the

alloys with a smaller number of elements has a stronger tendency to increase structural ordering, whereas the reverse is observed for alloys with $n \geqslant 7$. The phenomenon reflects the competition between the dense packing (for lowering enthalpy energy) and the randomness of atoms (for increasing configurational entropy and $T\Delta S$) driven by thermal energy. In each step during simulation, each jumping atom is to seek its minimum-energy position under the rule of minimizing energy. But, at the same time, the kinetic energy or momentum also drives atoms to jump, which is against the tendency towards the minimum energy. Since the jumping becomes larger at high temperatures, it becomes dominant in making the atomic configuration more disordered. This can be interpreted as the high-entropy effect, which is enhanced at high temperatures [2].

5. Concluding remarks

Rapidly solidified structure of alloys with equal-molar elements composed of up to eight elements (Ni–Al–Cu–Co–Ti–V–Zn–Zr) has been modeled for the first time using molecular dynamic simulation. According to the RDF curves obtained, the melt-quenched alloys with increasing number of elements (n) show amorphous ($n \leqslant 4$) and liquid-like ($n \geqslant 5$) structures, respectively. This indicates that the degree of disorder increases with n. Quantitative analysis of the RDF curves gave the values R_2/R_1 and R_3/R_1, which reveal that the melt-quenched alloys with $n \leqslant 4$ tend to form amorphous solids, while alloys with $n \geqslant 5$ form liquid-like solids. After annealing at 900 K, the alloys with $n \leqslant 6$ keep amorphous structure but with a higher degree of order, while those with $n = 7$ and 8 become even more random than their original quenched state. The hard ball close-packing model is proposed to explain the evolution of amorphous and liquid-like structures, and their RDF features, in which the merging of the third and fourth shells and/or that of the second and third shells are the key for the judgment. In addition, the competition between the dense packing (for lowering enthalpy energy) and the randomness of atoms (for increasing $T\Delta S$) driven by thermal energy is proposed to elucidate the effect of annealing on atomic configuration. Since the effect of configurational entropy becomes more important at higher temperatures, a higher degree of randomness among different kinds of atoms is expected for the annealing states at higher temperatures.

Acknowledgment

The authors are grateful to the National Science Council of Taiwan, ROC, for the sponsorship of the current work under contract number NSC-95-2120-M-007-004.

References

[1] Huang K H 1995 A study on the multi-component alloy systems containing equal-mole elements *Master Degree Thesis* National Tsing Hua University in Taiwan
[2] Yeh J W, Chen S K, Lin S J, Gan J Y, Chin T S, Shun T T, Tsai C H and Chang S Y 2004 *Adv. Eng. Mater.* **6** 299
[3] Huang P K, Yeh J W, Shun T T and Chen S K 2004 *Adv. Eng. Mater.* **6** 74
[4] Hsu C Y, Yeh J W, Chen S K and Shun T T 2004 *Metall. Mater. Trans.* A **31** 1465
[5] Haile J M 1997 *Molecular Dynamics Simulation: Elementary Methods* (New York: Wiley)
[6] Yeh J W, Chen S K, Gan J Y, Lin S J, Chin T S, Shun T T, Tsau C H and Chang S Y 2004 *Metall. Mater. Trans.* A **35** 2533
[7] Chen T K, Shun T T, Yeh J W and Wong M S 2004 *Surf. Coat. Technol.* **188** 193
[8] Tong C J, Chen Y L, Chen S K, Yeh J W, Shun T T, Tsau C H, Lin S J and Chang S Y 2005 *Metall. Mater. Trans.* A **36** 881
[9] Tong C J, Chen M R, Chen S K, Yeh J W, Shun T T, Lin S J and Chang S Y 2005 *Metall. Mater. Trans.* A **36** 1263
[10] Chen Y Y, Duval T, Hung U D, Yeh J W and Shih H C 2005 *Corros. Sci.* **47** 2257
[11] Chen Y Y, Hong U T, Shih H C, Yeh J W and Duval T 2005 *Corros. Sci.* **47** 2679
[12] Chen Y Y, Hong U T, Yeh J W and Shih H C 2005 *Appl. Phys. Lett.* **87** 261918
[13] Chen T K, Wong M S, Shun T T and Yeh J W 2005 *Surf. Coat. Technol.* **200** 1361
[14] Chen Y Y, Hong U T, Shih H C and Yeh J W 2006 *Scr. Mater.* **54** 1997
[15] Chen M R, Lin S J, Yeh J W, Chen S K, Huang Y S and Chuang M H 2006 *Metall. Mater. Trans.* A **37A** 1363
[16] Chen M R, Lin S J, Yeh J W, Chen S K, Huang Y S and Tu C P 2006 *Mater. Trans.* **47** 1395
[17] Wu J M, Lin S J, Yeh J W, Chen S K, Huang Y S and Chen H C 2006 *Wear* **261** 513
[18] Tomanek D, Aliigia A A and Balseiro C A 1985 *Phys. Rev.* B **32** 5051
[19] Cleri F and Rosato V 1993 *Phys. Rev.* B **48** 22
[20] Duan G, Xu D, Zhang Q, Zhang G, Cagin T, Johnson W L and Goddard W A III 2005 *Phys. Rev.* B **71** 224208
[21] Ferrando R and Tréglia G 1995 *Surf. Sci.* **331** 920
[22] Guerdane M and Teichler H 2001 *Phys. Rev.* B **65** 014203
[23] Waseda Y 1980 *The Structure of Non-Crystalline Materials* (New York: McGraw-Hill) pp 90–3
[24] Elliott S R 1990 *Physics of Amorphous Materials* 2nd edn (England: Longman Scientific & Technical) pp 1–27
[25] Luborsky F E 1983 *Amorphous Metallic Alloys* (England: Butterworths) pp 8–25
[26] Ding K and Andersen H C 1986 *Phys. Rev.* B **34** 6987
[27] Turnbull D 1977 *Scr. Mater.* **11** 1131
[28] Turnbull D 1981 *Metall. Trans.* B **12B** 217
[29] Lindsay Greer A 1993 *Nature* **366** 303
[30] Elliott S R 1990 *Physics of Amorphous Materials* 2nd edn (England: Longman Scientific & Technical) pp 152–7
[31] Sheng H W, Luo W K, Alamgir F M, Bai J M and Ma E 2006 *Nature* **439** 419
[32] Miracle D B, Lord E A and Ranganathan S 2006 *Mater. Trans.* **47** 1737
[33] Miracle D B, Egami T, Flores K M and Kelton K F 2007 *MRS Bull.* **32** 629